Oxygen Potential Measurement of Iron Silicate Slag-Copper-Matte System

Yoichi Takeda

Associate Professor, Department of Materials Science and Technology, Faculty of Engineering, Iwate University, Ueda 4-3-5, Morioka 020, Japan.
Tel. 81-196-21-6367, Fax. 81-196-21-6373

ABSTRACT

The phase stability diagrams for the Cu-Fe-O-S-SiO_2 are illustrated at 1473 and 1573K. To collect the information for arranging the diagrams, several kinds of equilibrium experiments such as slag-copper metal, slag-matte, and slag-matte-copper metal are performed with an oxygen sensor to measure oxygen potential in the system. The data are presented in the diagrams of log P_{02} or log P_{S2} vs. $1/T$ and log P_{02} vs. log P_{S2}.

1. INTRODUCTION

The quinary system of Cu-Fe-O-S-SiO_2 is essential system in copper smelting. Concentrate usually contains copper, iron oxygen and sulfur, and oxygen is also an useful reactant from air. We add silica as flux to avoid the mutual miscibility between slag and matte and to make slag melt at smelting temperature. In copper matte smelting furnace, sulfur reacts with oxygen and separates as sulfur dioxide to gas phase, and iron oxidizes and separates to slag phase, and consequently copper concentrates in matte phase, that is further oxidized and converted to blister copper. I have carried out several kinds of equilibrium experiment including slag, matte or copper melt. In the experiments immersing an oxygen sensor in the melt, I have measured oxygen potential in the system. The experimental data are available for illustrating a phase stability. The phase stability diagram of the Cu-Fe-O-S-SiO_2 give us important information to comprehend the condition of copper smelting steps thermodynamically. In order to arrange a fundamental experimental research for copper smelting and analyze the experimental data, the diagram is also helpful to us. Portrayal of the phase relationships in the quinary system of Cu-Fe-O-S-SiO_2 requires consideration of 10 binary, 10 ternary and 5 quaternary sub-systems for which the information is fragmentary in many cases[1], especially in over quaternary. We have performed several kind of equilibrium experiments. I illustrate phase stability diagrams combining the experimental data and information from literature. Several ways to describe a phase stability diagram have been proposed, and each of them has advantage and disadvantage. I present the univariant equilibria including the sub-system of the quinary system on the diagrams of lop P_{02} and lop P_{S2} vs. $1/T$. The phase stability diagrams for the quinary system of Cu-Fe-O-S-SiO_2 are illustrated on the lop P_{02} vs. lop P_{S2} plane which diagram has been presented by Yazawa[2].

2. EXPERIMENTS

There are many phase combination in the quinary system including molten phase. Simple one is slag-metal equilibrium which has been presented in another paper[3]. The equilibrium experiment among slag, matte and copper metal phase under iron saturation provided also useful information for us[4]. In the experiment oxygen potential was measured, and sulfur potential and the activity of copper were estimated from metal composition. I present the following three kind experimental data; equilibrium between slag and matte in the Fe-S-O-SiO_2 system under iron saturation, equilibrium between slag and matte of the Fe-Cu-S-O-SiO_2 system under 10% and 100% SO_2 atmosphere in a magnesia crucible, and equilibrium among slag, matte and copper metal in a magnesia crucible.

2.1 Slag-matte equilibrium in the Fe-S-O-SiO_2 system

FeO-SiO_2 slag and Fe-S matte are melted in an iron crucibles at 1473 and 1573K. Oxygen potential in the melt is measured with an oxygen sensor. The slag and matte compositions in the quenched samples are determined by chemical analysis. Oxygen, sulfur and iron contents in the matte phase, on mass per cent base, at 1473K are shown in Fig. 1 and Fig. 2 against oxygen partial pressure. Silica, iron and sulfur contents in the slag phase are also shown in Fig. 3. Closed marks in the figure show the experimental result for slag-matte equilibrium in the Fe-S-O-SiO_2 system. As further reference experiment Fe-S-O matte is melted in an iron crucible and oxygen potential is also measured. The results are shown in the figures with open marks. As the matte composition in the slag-matte equilibrium is very close to the Fe-S-O matte under iron saturation at a given oxygen potential, sulfur potential in both system will be close to each other. The sulfur partial pressure in Figure 2 is calculated by the Gibbs-Duhem integration for Fe-S-O system under unity of iron activity. Steep increase in sulfur content in the slag is observed with decreasing oxygen partial pressure and silica content in slag, and slag and matte does not separate at critical point of 10% SiO_2. The experimental results at 1573K for the same system are plotted on Figs 4, 5 and 6.

2.2 Slag-matte equilibrium under SO_2 atmosphere

Slag and matte in the Fe-Cu-S-O-SiO_2 system is equilibrated with 10 or 100% SO_2 gas phase in a magnesia crucible under controlled S_2 partial pressure at 1473 and 1573K. The oxygen potential in the system is measured by immersing an oxygen sensor. Magnesia content in slag dissolved from a crucible is 5 to 9%. The experimental detail is described in the other paper[5] in this proceedings. The oxygen partial presser, P_{02}/atm., is plotted against the iron content in matte, {%Fe} on mass per cent base, as Fig. 7. Although sulfur partial pressure in the gas phase is controlled, it is difficult to equilibrate molten phases with gas phase in sulfur potential, hence sulfur partial pressure, P_{S2}/atm., is calculated from the measured oxygen potential by equation (3) and shown in Fig. 7.

$$1/2\ S_2(g) + O_2(g) = SO_2(g) \qquad (1)$$

$$\Delta G^\circ/\mathrm{J} = -362000 + 73.136T \ ^{6} \qquad (2)$$

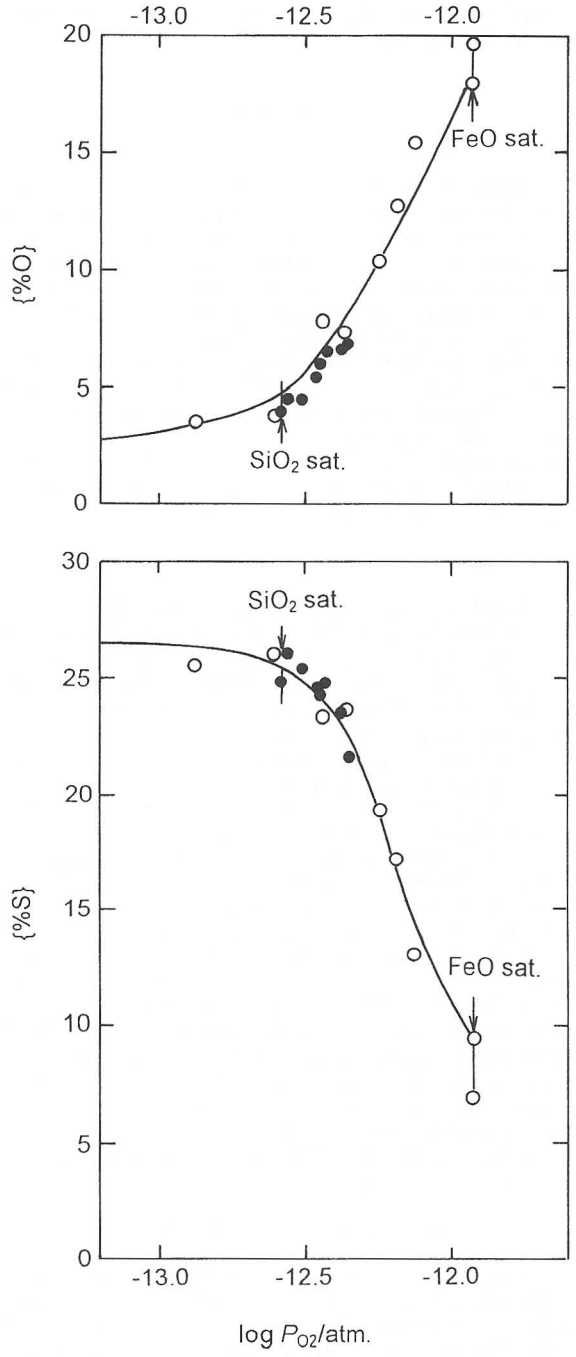

Fig. 1. Oxygen, and sulfur contents in matte under iron saturation at 1473K. Open circle shows those in the Fe-S-O system, and closed circle does for the slag-matte equilibrium in the Fe-S-O-SiO_2 system.

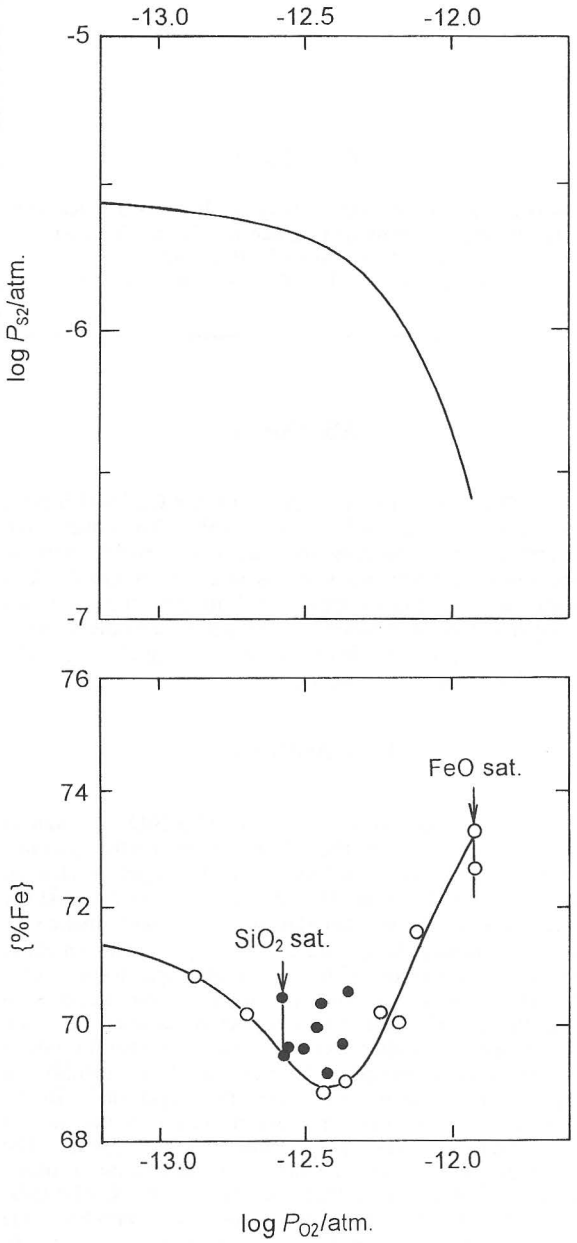

Fig. 2. Calculated sulfur partial pressure by the Gibbs-Duhem integration, the top figure, and iron content in matte , the bottom figure, under iron saturation at 1473K.

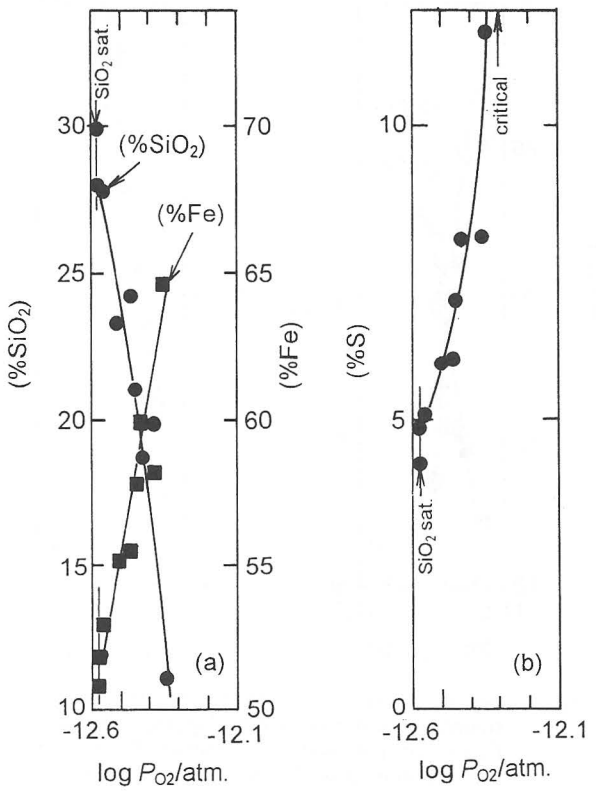

Fig. 3. Silica and iron contents in slag, the left side figure, and sulfur content in slag, the right side figure, for slag- matte equilibrium in the Fe-S-O-SiO_2 system under iron saturation at 1473K.

$$\log P_{O2}/\text{atm.} = \log P_{SO2} - 1/2 \log P_{S2} - 18908/T + 3.82 \quad (3)$$

Linear relations of $\log P_{O2}$ or $\log P_{S2}$ against log{%Fe} are observed in Fig. 7. {%Fe} is related to copper content in matte, {%Cu}, by equation (4) under higher SO_2 atmosphere.

$$\{\%Fe\} = 65.5 - 0.824\ \{\%Cu\} \quad (4)$$

2.3 Slag-matte-copper metal equilibrium

Slag containing 18 to 21% SiO_2 or 28 to 33% SiO_2 is melted with matte and copper metal in a magnesia crucible at 1573K. The oxygen partial pressure is measured with an oxygen sensor and plotted against iron or copper content in matte as shown in Fig. 8. In this phase equilibrium, sulfur dioxide partial pressure increases from 10^{-6} atm. to 0.1 atm. with increasing oxygen partial pressure.

3. PHASE STABILITY DIAGRAM

3.1 Univariant equilibria in the related system

There are many univariant equilibria in the Cu-Fe-O-

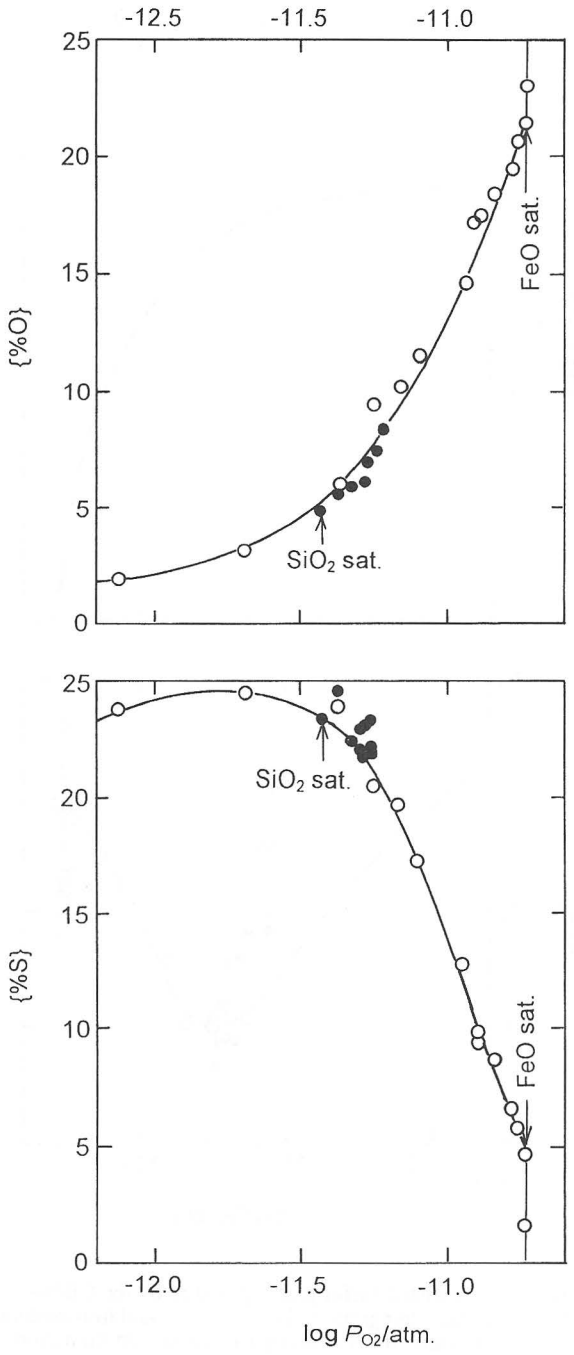

Fig. 4. Oxygen, and sulfur contents in matte under iron saturation at 1573K. Open circle shows those in the Fe-S-O system, and closed circle does for the slag-matte equilibrium in the Fe-S-O-SiO_2 system.

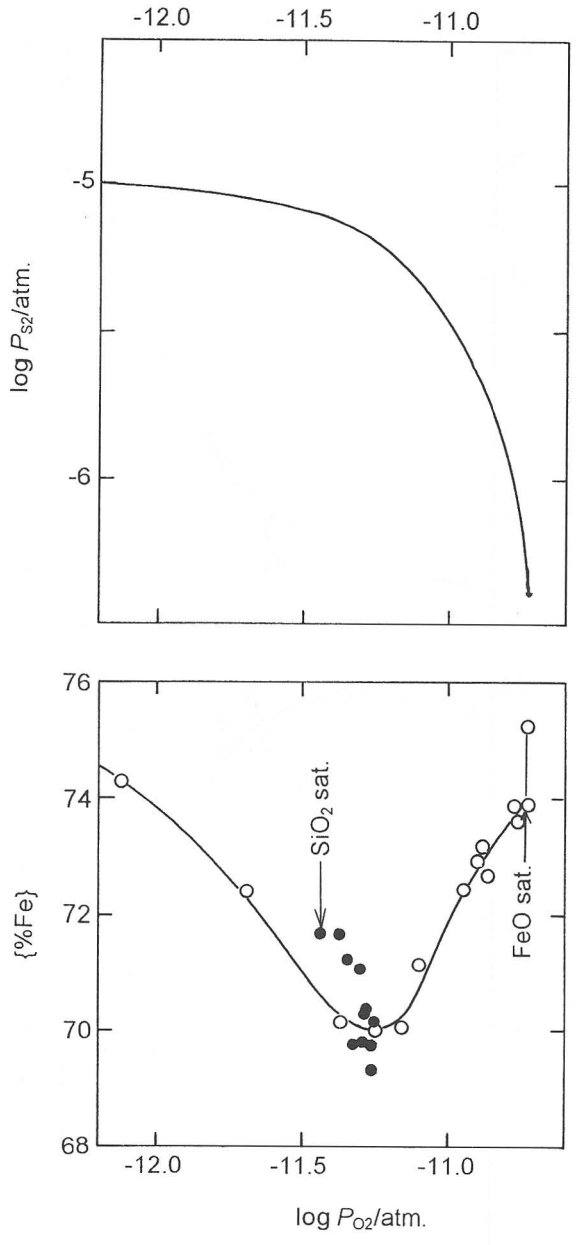

Fig. 5. Calculated sulfur partial pressure by the Gibbs-Duhem integration, the top figure, and iron content in matte , the bottom figure, under iron saturation at 1573K.

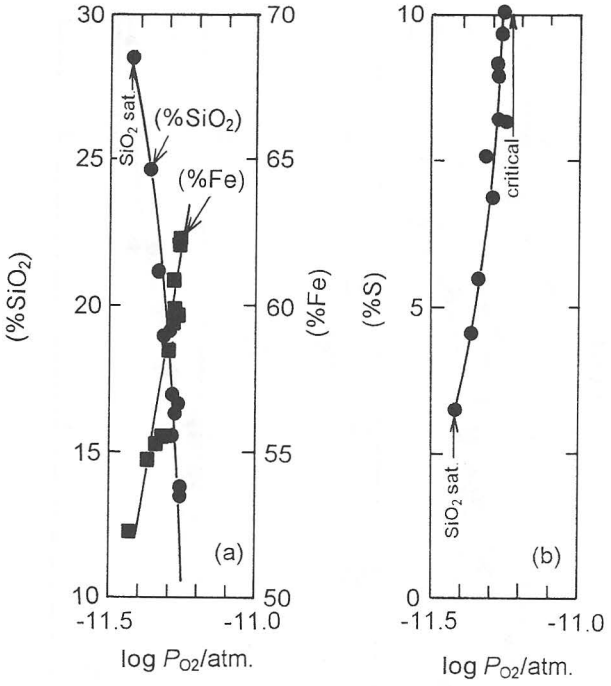

Fig. 6. Silica and iron contents in slag, the left side figure, and sulfur content in slag, the right side figure, for slag- matte equilibrium in the Fe-S-O-SiO_2 system under iron saturation at 1573K.

S-SiO_2 quinary system and its sub-systems. Essential one to comprehend copper smelting with iron silicate slag is listed in Table I. For the sake of saving space in the table, equilibrium phase is shown by molecular expression and sometimes minor species in the phase is eliminated. The oxygen partial pressures in univariant equilibria are shown in Fig. 9 against reciprocal temperature, $1/T$. The symbol beside line in the figure correspond with that in Table I. Marked **h** is univariant equilibrating solid iron with wustite in Fe-O binary, and **j** is an univariant equilibrium of solid iron-silica-iron silicate slag in Fe-O-SiO_2. There are many univariant equilibria in the Cu-Fe-O-S-SiO_2 between **h** and **j**, so the figure axes are expanded in this region as shown in Fig. 10. The sulfur partial pressures in univariant equilibria are also shown in Fig. 11.

3.2 Phase stability diagram under iron saturation

Phase stability diagrams in the Cu-Fe-O-S-SiO_2 system at 1573 and 1473K are illustrated in Figs 12 and 13. In the figure solid iron is oxidized or sulfidized and disappears on the upper area on the line connecting points **g**, **C**, **E**,**G** and **α**. Under the line connecting points **i**, **F** and **G** iron oxide in slag is reduced and slag phase disappears. The line connecting **D** to **E** is critical that slag and matte do not separate and form oxysulfide containing considerable amount of oxygen and sulfur. Silica content in slag is around 10 to 15% and copper content in matte is less than 15 at the critical composition. Copper content in matte saturated copper metal, on the line of **γ**, **F**, **D**, decreases from 52 to 15% at 1573K and from 56% to 15% at 1473K with increasing oxygen partial pressure. Oxygen content in the matte increases from 0 to 15%. Following nine molten phase equilibria in the quinary system are possible under solid iron saturation; slag, copper metal, matte, oxysulfide, slag-copper metal, oxysulfide-copper metal, slag-matte-copper metal, matte-copper metal, slag-matte.

Table I Oxygen and sulfur partial pressures for univariant equilibria in related systems

Symbol	System	Condensed phase	log P_{O2}/atm.	log P_{S2}/atm.	Refernce
a_1-a_2	Cu-O	Cu(l), Cu_2O(l)	5.629-14290/*T*		
a_1	Cu-O	Critical point at 1608K			
a_2	Cu-O	Cu(l), Cu_2O(l), Cu_2O(s); Monotectic at 1489K			
a_2-a_3	Cu-O	Cu(l), Cu_2O(s)	10.130-21000/*T*		7
b	Cu-O-SiO_2	Cu(l), SiO_2(s), (Cu_2O-SiO_2)slag	3.70-11630/*T*		8
c	Cu-Fe-O-SiO_2	Cu(l), SiO_2(s), Fe_3O_4(s), (Cu_2O-FeO_x-SiO_2)slag			
d	Cu-Fe-O-SiO_2	Cu(l), SiO_2(s), Fe_3O_4(s), (FeO_x-SiO_2)slag			
e	Fe-O-SiO_2	SiO_2(s), Fe_3O_4(s), (FeO_x-SiO_2)slag	25.11-48840/*T*		9
f	Fe-O	FeO(s), Fe_3O_4(s)	15.08-35810/*T*		10
g	Fe-Cu-O-SiO_2	Fe(s), FeO(s), Cu(l), (FeO-SiO_2)slag	6.45-26920/*T*		
h	Fe-O	Fe(s), FeO(s)	6.77-27520/*T*		11
i	Fe-Cu-O-SiO_2	Fe(s), SiO_2(s), Cu(l), (FeO-SiO_2)slag	2.94-22500/*T*		
j	Fe-O-SiO_2	Fe(s), SiO_2(s), (FeO-SiO_2)slag	3.67-23810/*T*		10
α	Fe-S	Fe(s), (Fe-S)matte		2.93-12360/*T*	
β-β_2	Cu-S	Cu(l), Cu_2S(l)		4.76-15900/*T*	12
β_2-β_3	Cu-S	Cu(l), Cu_2S(s)			
γ	Fe-Cu-S	Fe(s), Cu(l), (Cu-Fe-S)matte		3.67-14660/*T*	13, 14, 15
A	Fe-S-O-SiO_2	SiO_2(s), (Fe-S-O)matte, slag, 1 atm. SO_2	2.60-16200/*T*	2.39-5320/*T*	
B	Fe-S-O-SiO_2	SiO_2(s), (Fe-S-O)matte, slag, 0.1 atm. SO_2	1.95-16200/*T*	1.23-4630/*T*	
A'	Fe-Cu-S-O-SiO_2	SiO_2(s), Cu(l), Cu_2S(l), slag, 1 atm. SO_2	1.86-11570/*T*	4.76-15900/*T*	
B'	Fe-Cu-S-O-SiO_2	SiO_2(s), Cu(l), Cu_2S(l), slag, 0.1 atm. SO_2	3.65-15740/*T*	4.76-15900/*T*	
C	Fe-S-O	Fe(s), FeO(s), (Fe-S-O)matte	68.9-27710/*T*	-3.53-4490/*T*	
D	Fe-Cu-S-O-SiO_2	Fe(s), Cu(l), matte, slag, oxysulfide; Critical point	4.84-24770/*T*	2.73-13890/*T*	
E	Fe-S-O-SiO_2	Fe(s), matte, slag, oxysulfide; Critical point	4.80-25230/*T*	3.34-13430/*T*	
F	Fe-Cu-S-O-SiO_2	Fe(s), Cu(l), SiO_2(s), matte, slag	3.93-24070/*T*	3.72-15050/*T*	
G	Fe-S-O-SiO_2	Fe(s), SiO_2(s), matte, slag	5.18-26160//*T*	2.83-12500/*T*	

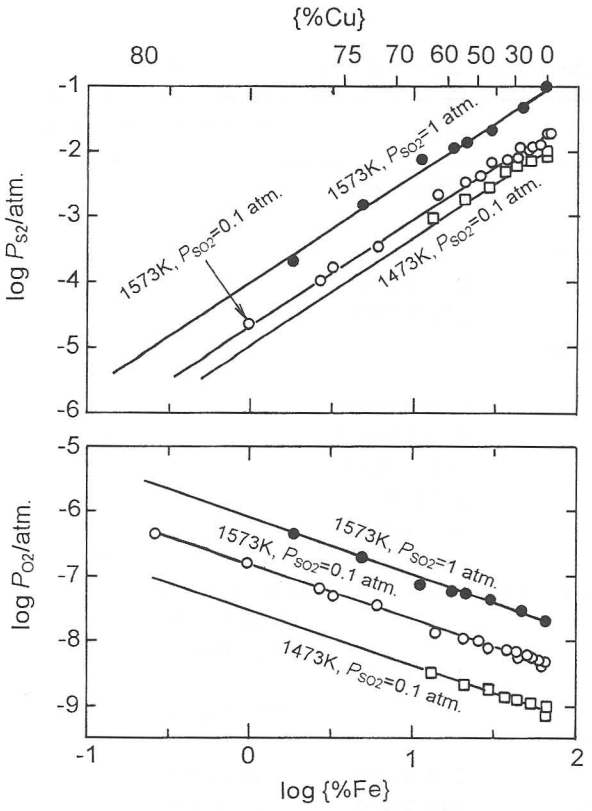

Fig. 7. Oxygen and sulfur partial pressure for slag-matte equilibrium with 0.1 or 1 atm. SO_2 pressure at 1473 or 1573K against iron content in matte. Silica saturated FeO_x-SiO_2 slag and matte are melted in a magnesia crucible.

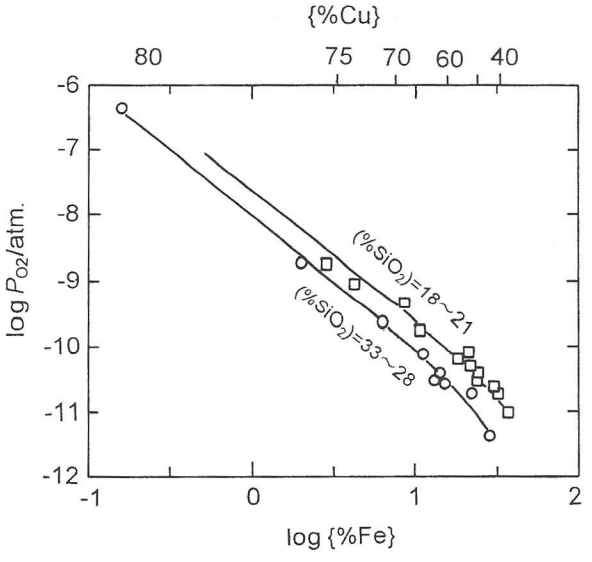

Fig. 8. Oxygen partial pressure for slag-matte-copper metal equilibrium at 1573K. FeO_x-SiO_2 slag containing 18 to 21% SiO_2 or 28 to 32% SiO_2, matte and copper metal are melted in a magnesia crucible.

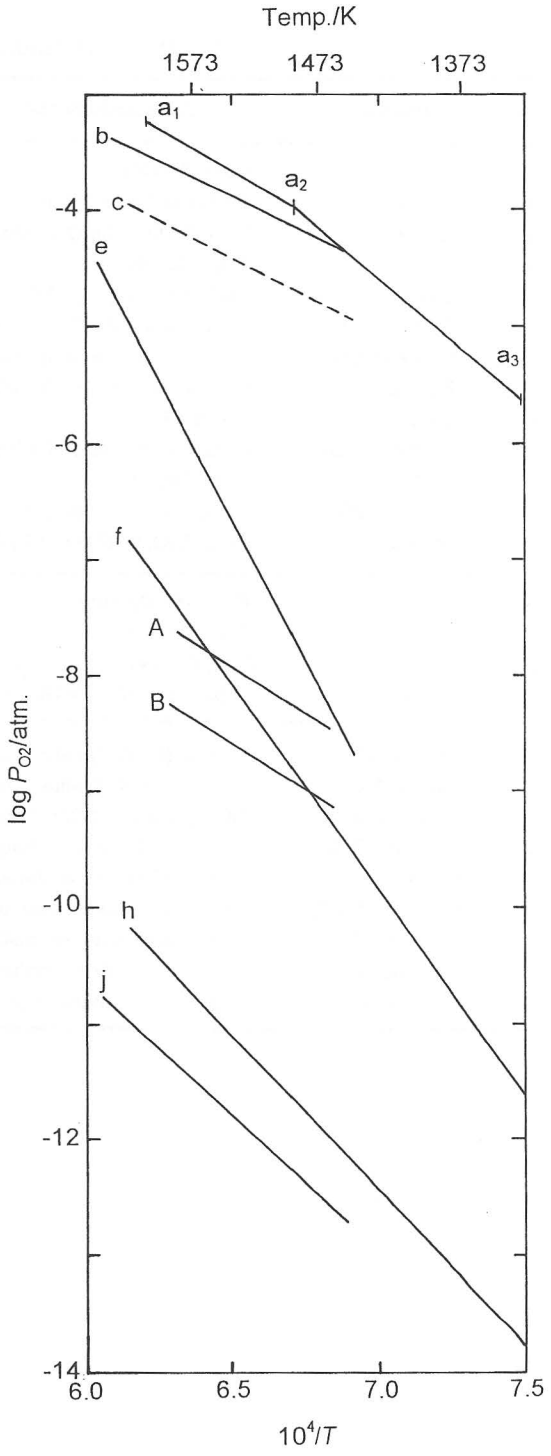

Fig. 9. Oxygen partial pressure for univariant equilibria in the Fe-Cu-S-O-SiO_2 and its sub-systems.

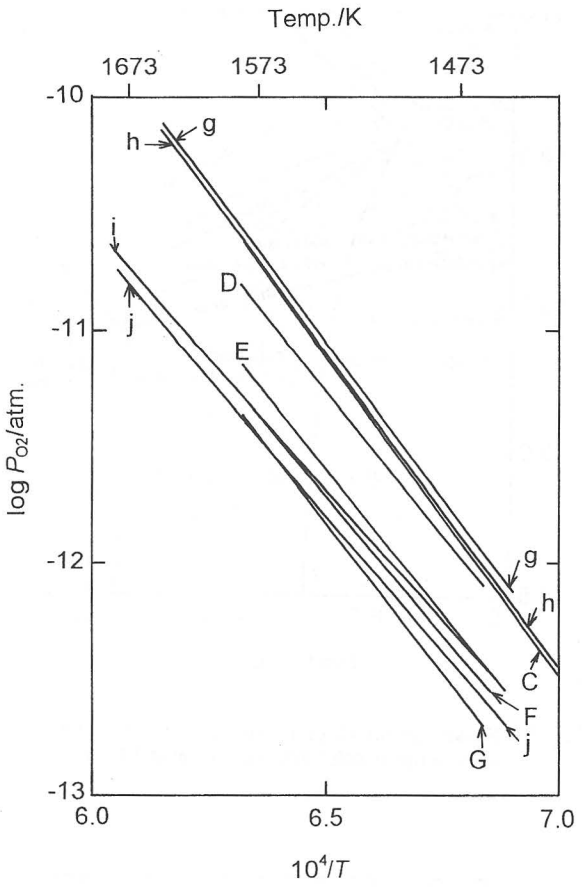

Fig. 10. Oxygen partial pressure for univariant equilibria in the Fe-Cu-S-O-SiO_2 and its sub-systems under solid iron saturation.

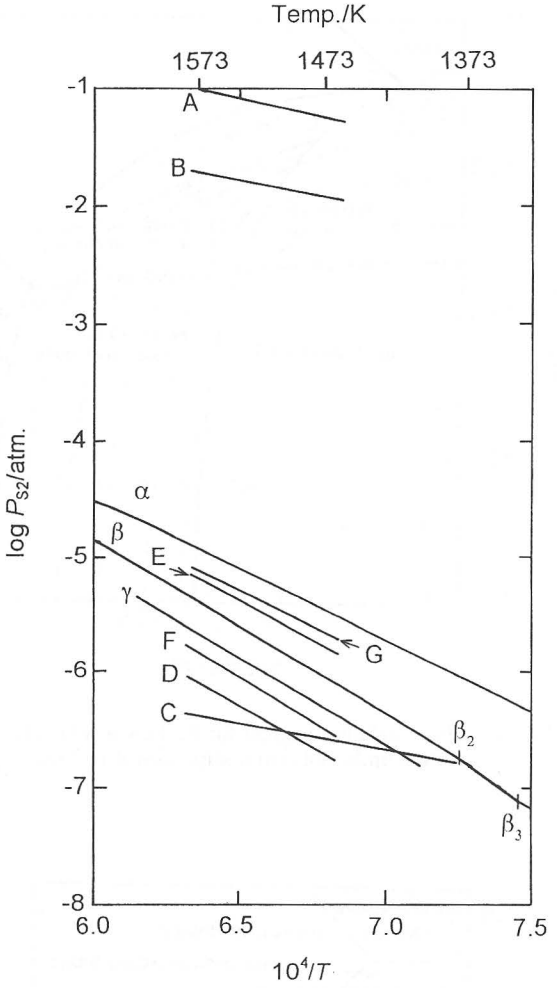

Fig. 11. Sulfur partial pressure for univariant equilibria in the Fe-Cu-S-O-SiO_2 and its sub-systems.

3.3 Phase stability diagram in copper smelting condition

Phase stability diagrams in more wide range of oxygen and sulfur partial pressures are illustrated in Figs 14, 15 and 16 to comprehend copper smelting condition thermodynamically. The lines which show constant copper content in matte are based on the information of slag-matte equilibrium experiment melted in a magnesia crucible. Fig. 14 and Fig. 16 are illustrated under the condition of silica saturation at 1573 and 1473K, respectively, and Fig. 15 is under 20% SiO_2 in slag at 1573K. Decrease in silica content in slag, increase in iron content, leads to high oxygen pressure at given copper content in slag and sulfur dioxide partial pressure. Fig. 14, that is under silica saturation at 1573K, is not essentially different from that presented by Yazawa[2] because the affinities between the components in the quinary system are unique and decided by Heaven. If we see some difference in the figures, that is due to an experimental error or human mistake. We can get large amount of important information from a phase stability diagram. It is necessary for well understanding the diagram to contrast its composition diagram.

4. CONCLUSION

Oxygen and sulfur partial pressures for univariant equilibria in the Cu-Fe-O-S-SiO_2 system and its related sub-system are presented. The phase stability diagrams for the Cu-Fe-O-S-SiO_2 system, under silica saturation and 20% SiO_2 at 1473 and 1573K, are illustrated to comprehend copper smelting condition.

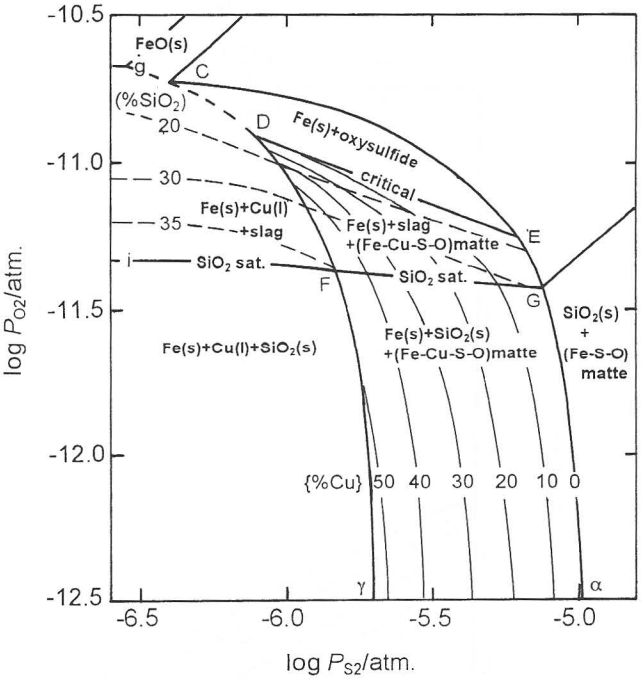

Fig. 12. Phase stability diagram for the Fe-Cu-S-O-SiO_2 system under solid iron saturation at 1573K.

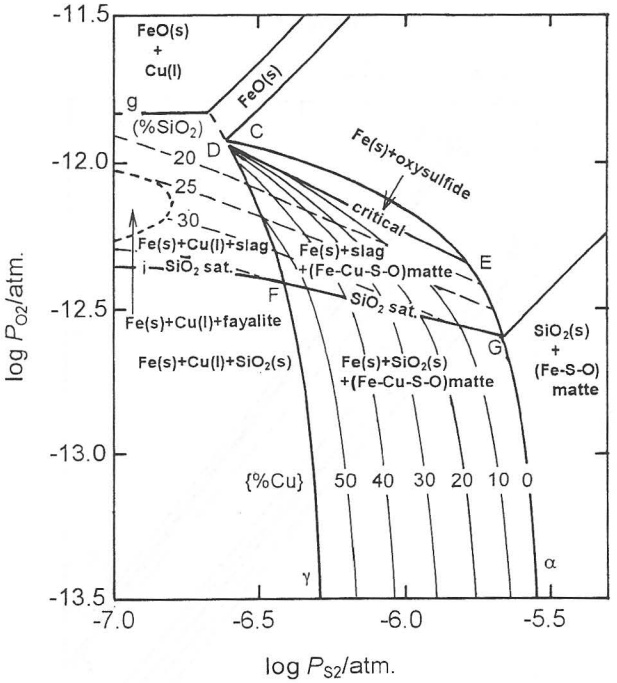

Fig. 13. Phase stability diagram for the Fe-Cu-S-O-SiO_2 system under solid iron saturation at 1473K.

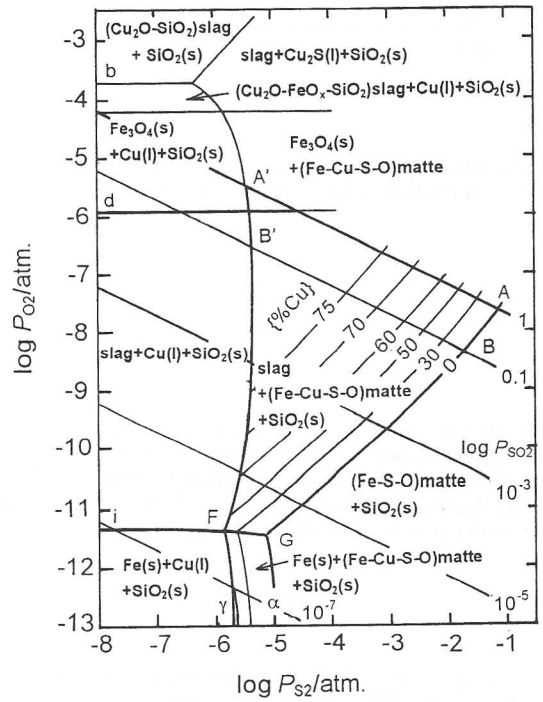

Fig. 14. Phase stability diagram for the Fe-Cu-S-O-SiO_2 system under solid silica saturation at 1573K.

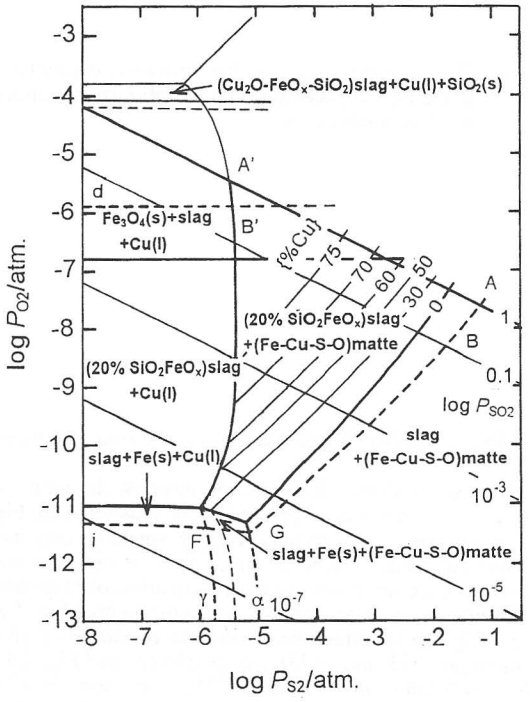

Fig. 15. Phase stability diagram for the Fe-Cu-S-O-SiO_2 system with 20% SiO_2 slag at 1573K.

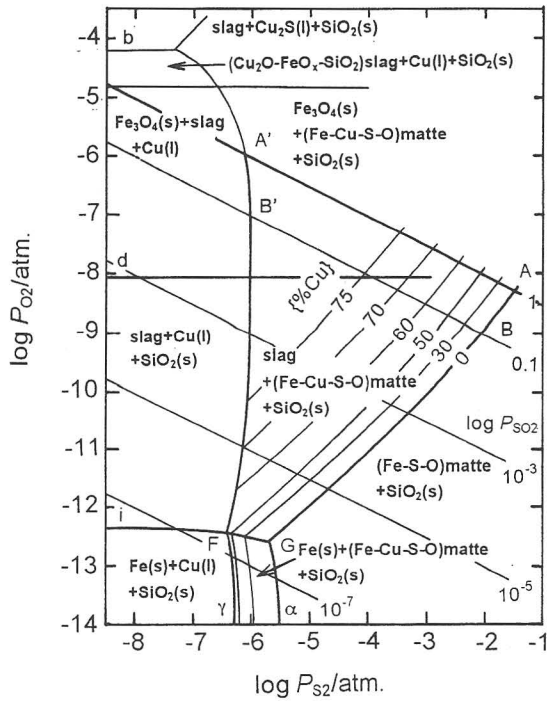

Fig. 16. Phase stability diagram for the Fe-Cu-S-O-SiO_2 system under solid silica saturation at 1473K.

REFERENCES

1. J.F. Elliott, "Phase Relationships in the Pyrometallurgy of Copper", Metall. Trans., Vol. 7B, March, 1976, pp.17-33.

2. A. Yazawa, "Thermodynamic Considerations of Copper Smelting", Can. Met. Quart., Vol. 13, No.3, 1974, pp.443-453.

3. Y. Takeda, "The Effects of Basicity on Oxidic Dissolution of Copper in Slag", Metallurgical Processes for the Early Twenty-First Century, TMS, Vol. 1, 1994, pp.453-466.

4. Y. Takeda, "Oxidic and Sulfidic Dissolution of Copper in Matte Smelting Slag", Proceedings of 4th International Conference on Molten Slags and Fluxes, ISIJ, 1992, pp.584-589.

5. Y. Takeda, "Copper Solubility in Matte Smelting Slag", 5th International Conference on Molten Slags, Fluxes and Salts '97, ISS, 1997.

6. J.P. Coughlin, "Contributions to the Data on Theoretical Metallurgy", Bureau of Mines, Bulletin 542.

7. Y. Kayahara, "Thermodynamic Study of the Liquid Cu-O system", Trans. JIM, Vol. 22, No. 7, 1981, pp.493-500.

8. U. Kuxmann and K. Kurre, "Die Mischungslücke im Kupfer-Sauerstoff und ihre Beeinflussung durch die Oxide CaO, SiO_2, Al_2O_3, MgO· Al_2O_3 und ZrO_2", Erzmetall, Vol. 21, 1968, pp.199-209.

9. E.J. Michal and R. Schuhmann, "Thermodynamics of Iron-Silicate Slags: Slags Saturated with Solid Silica", Trans. AIME, Vol. 194, 1952, pp.723-728.

10. E. Schürmann and G. Kraume, "Reduktionsgleeich-gewichte im System Fe-Fe_2O_3-CaO oberhalb 1050°C", Arck. Eisenhüttenwes., Vol. 47, No. 9, 1976, pp.471-476.

11. G.G. Charette and S.N. Flengas, "Thermodynamic Properties of the Oxides of Fe, Ni, Pb, Cu and Mn, by EMF Measurements", J. Electrochem. Soc., Vol. 115, No. 8, 1968, pp.796-804.

12. J. Niemelä and P. Taskinen, "Activities and Phase Equilibria in Cu-S Melts by EMF Techniques", Scand. J. Metall., Vol. 13, 1984, pp.382-390.

13. W.A. Krivsky and R. Schuhmann, "Thermodynamics of the Cu-Fe-S System at Matte Smelting Temperatures", Trans. AIME, Vol. 209, 1957, pp. 988-981.

14. Y.A. Chang, J.P. Neumann and U.V. Choudary, "Phase Diagrams and Thermodynamic Properties of Ternary Copper-Sulfur-Metal Systems". INCRA Monograph VII, NSRDS, 1979, pp.58-88.

15. J. Koh and A. Yazawa, "Thermodynamic Properties of the Cu-S, Fe-S and Cu-Fe-S Systems", Bulletin of the Research Institute of Mineral Dressing and Metallurgy, Tohoku University, Vol. 38, No. 2, 1982, pp. 107-118.